

Photopolymerization in the Fullerene Layers of the Molecular Donor–Acceptor Complex $\{\text{Pt}(n\text{Pr}_2\text{dte})_2\} \cdot (\text{C}_{60})_2$

K. P. Meletov

Institute of Solid State Physics, Russian Academy of Sciences, Chernogolovka, Moscow oblast, 142432 Russia

e-mail: mele@issp.ac.ru

Received April 26, 2018

Abstract—We measured Raman spectra in crystals of molecular donor–acceptor fullerene complexes $\{\text{Me}(n\text{Pr}_2\text{dte})_2\} \cdot (\text{C}_{60})_2$ ($\text{Me} = \text{Ni}, \text{Cu}, \text{Pt}$). In the spectra of the $\{\text{Pt}(n\text{Pr}_2\text{dte})_2\} \cdot (\text{C}_{60})_2$ complex under prolonged irradiation with a laser with $\lambda = 532$ nm, characteristic changes in the photopolymerization of fullerene are observed, associated with the splitting of degenerate phonon Hg modes and softening of Ag modes of the C_{60} molecule. The kinetics of photopolymerization under conditions of weak irradiation at room temperature is studied. It was found that thermal destruction of the photopolymer with increasing temperature leads to a decrease in its concentration in the final photopolymerization product. The kinetics of thermal destruction is described by the Arrhenius equation, with the activation energy E_A of (0.68 ± 0.03) eV; the dimers are destructed to a concentration of 1% within 15 min at $\sim 114^\circ\text{C}$.

DOI: 10.1134/S1063783418100190

1. INTRODUCTION

The synthesis of the donor–acceptor complexes of fullerene and the study of their crystal structure and electrical, magnetic, and optical properties at normal and high pressures is of considerable interest [1–7]. Complexes have a layered structure where the fullerene layers alternate with the layers of the molecular donor, which can be aromatic hydrocarbons, tetra-thiofulvalenes, amines, metalloporphins, metallo-cenes, and others, and the interaction between the molecules in the layers and between the layers is of a van der Waals nature. The investigation of complexes at high pressures is of considerable interest, because the energy spectrum and properties of crystals with the van der Waals interaction are very sensitive to changes in intermolecular distances. The overlap of the electron clouds of the HOMO level of the donor and the LUMO level of the acceptor increases with increasing pressure and can lead to charge transfer, especially if the complexes under normal conditions are close to ionic. At the same time, a decrease in the distances between fullerene molecules at high pressure can stimulate the formation of covalent bonds between them since these distances are small at normal pressure.

Indeed, the Raman spectra of molecular complexes of fullerene at high pressure show abrupt changes in the pressure dependence of the phonon modes [3–8]. Such changes were first observed in measurements of Raman spectra of the fullerene complex with tetramethyltetraselenefulvalene $\{\text{C}_{10}\text{H}_{12}\text{Se}_4(\text{CS}_2)_2\} \cdot \text{C}_{60}$ at 5 GPa, accompanied by

splitting of degenerate Hg modes and softening of nondegenerate Ag intramolecular C_{60} modes [6]. Similar changes were observed in the Raman spectra of the molecular complex $\text{C}_{60} \cdot \{\text{Fe}(\text{C}_5\text{H}_5)_2\}_2$ ($\text{Fe}(\text{C}_5\text{H}_5)_2$ is ferrocene) at a pressure of ~ 5 GPa, which were interpreted both as a charge transfer from the molecular donor to fullerene and by the formation of covalent bonds between molecules in the fullerene layers [3, 5]. Recently, changes in the Raman spectra of this complex were also observed at a pressure of ~ 2.8 GPa; these changes depended on the intensity and time of laser irradiation and were interpreted by the authors as pressure-stimulated photopolymerization in fullerene layers [4]. In our studies of the $\{\text{Hg}(\text{dedtc})_2\}_2 \cdot \text{C}_{60}$ complex ($\text{C}_{20}\text{H}_{40}\text{Hg}_2\text{N}_4\text{S}_8 \cdot \text{C}_{60}$ is fullerene with mercury diethyl dithiocarbamate), similar changes in Raman spectra were observed near ~ 2 GPa [7]. More detailed studies of the pressure dependence of the phonon modes and the crystal structure at high pressure were performed for the $\{\text{Cd}(\text{dedtc})_2\}_2 \cdot \text{C}_{60}$ complex [8]. It is found that changes in the Raman spectra of complexes at high pressure depend on the intensity and duration of irradiation with the laser light and are due to photopolymerization in the fullerene layers. It occurs only in the pressure range from 2 to 6 GPa, while outside this range up to 17 GPa, there are no similar changes in the spectra. At the same time, X-ray diffraction (XRD) data show that the distances between fullerene molecules in the complex at these pressures are greater than intermolecular distances in C_{60} crystalline polymers, and comparable distances

are attained at pressures >17 GPa [8]. Changes in the Raman spectra at ~ 2 GPa were also observed in $[\{\text{Cd}(\text{Et}_2\text{dte})\}_2 \cdot \text{DABCO}] \cdot \text{C}_{60} \cdot (\text{DABCO})_2$, but they disappeared when the wavelength of laser excitation varied from visible wavelength of $\lambda = 514$ nm to infrared wavelength of $\lambda = 785$ nm. The nature of the variation in the spectra under prolonged and intense exposure to visible light unambiguously attests to photopolymerization in the fullerene layers of the complex. This is confirmed by the XRD data, according to which no covalent bonds between C_{60} molecules are formed in this pressure range. Fullerene molecules are sufficiently far from each other, and the approximation of the pressure dependence of the parameters of the crystal lattice by the equation of state of the Mur-naghan type shows that the distances between them, characteristic of polymers, are attained only at a pressure >18 GPa [9]. Finally, in recent studies of the $\{\text{Pt}(\text{dbdtc})\}_2 \cdot \text{C}_{60}$ complex, photopolymerization in fullerene layers was observed for the first time at normal pressure, and a study of the stability of photooligomers at high temperature showed that they break at a lower temperature than photo- and crystalline polymers of C_{60} [10].

Polymerization of fullerene occurs during the formation of covalent bonds between molecules in fullerene crystals or films and is due to the presence of 30 unsaturated double $\text{C}=\text{C}$ bonds in the C_{60} molecule. When fullerene is irradiated with intense visible light, photopolymers C_{60} are formed [11]; ordered polymeric structures are formed by intercalation of C_{60} crystals with alkali metals [12] or by thermobaric treatment of fullerene under high pressure and temperature conditions [13, 14]. Covalent bonds between neighboring fullerene molecules arise as a result of a $[2 + 2]$ cycloaddition reaction upon the rupture of double $\text{C}=\text{C}$ bonds and the formation of single $\text{C}-\text{C}$ bonds between the carbon atoms of neighboring molecules. As a result, two carbon atoms with sp^3 hybridization appear in the fullerene molecule with sp^2 hybridization of all electronic orbitals. At the same time, a decrease in the symmetry of the molecule leads to the splitting of degenerate Hg modes, while a decrease in the stiffness of the skeleton of the molecule due to the disruption of double bonds leads to a softening of fully symmetric Ag modes [13–16]. In particular, the frequency of the most intense Ag(2) mode in the Raman spectra, corresponding to in-phase tangential vibrations of carbon atoms with simultaneous compression of the carbon pentagon and stretching of the hexagon, gradually decreases with increasing number of sp^3 -hybridized carbon atoms in the C_{60} molecule. This circumstance is widely used for rapid testing and determination of the type of crystalline fullerene polymers by optical spectroscopy in addition to structural analysis, and it is the only research tool for fullerene photopolymers.

In this study, Raman spectra were measured in crystals of molecular donor–acceptor fullerene com-

plexes $\{\text{Me}(n\text{Pr}_2\text{dte})\}_2 \cdot (\text{C}_{60})_2$ ($\text{Me} = \text{Ni}, \text{Cu}, \text{Pt}$) under normal pressure. It is shown that photopolymerization in the fullerene layers under visible laser irradiation is observed in the complex of fullerene with platinum bis(dipropyldithiocarbamate) $\{\text{Pt}(n\text{Pr}_2\text{dte})\}_2 \cdot (\text{C}_{60})_2$ (chemical formula $\text{C}_{14}\text{H}_{28}\text{PtN}_2\text{S}_4 \cdot \text{C}_{120}$), expressed in the splitting of Hg(1), Hg(3), Hg(4), Hg(7), and Hg(8) modes and softening of Ag(1) and Ag(2) modes, while similar changes are not observed in Raman spectra of the complexes with nickel and copper. The kinetics of photopolymerization was studied with the laser powers at the lowest possible to measure the Raman spectra and at temperatures up to 110°C . It is demonstrated that the active destruction of a photopolymer at high temperature leads to a decrease in its concentration in the final product obtained under conditions of photopolymerization saturation during prolonged irradiation. The kinetics of thermal destruction of the photopolymer is described by the Arrhenius equation, with the activation energy E_A of (0.68 ± 0.03) eV, and its destruction to a concentration of 1% occurs within 15 min at $\sim 114^\circ\text{C}$.

2. EXPERIMENTAL

The molecular complexes $\{\text{Me}(n\text{Pr}_2\text{dte})\}_2 \cdot (\text{C}_{60})_2$ ($\text{Me} = \text{Ni}, \text{Cu}, \text{Pt}$) (the chemical formula $\text{C}_{14}\text{H}_{28}\text{MeN}_2\text{S}_4 \cdot \text{C}_{120}$) were synthesized by slow evaporation of a solution containing fullerene and bis(dipropyldithiocarbamate) of the metal by the method described earlier [17]. Samples have the appearance of thin needle-shaped crystals of not very good quality, and their precise structural analysis is difficult. Structural analysis of such complexes shows that they have a layered structure in that the layers of fullerene C_{60} molecules alternate with the layers of a molecular donor. The molecules of fullerene in the complex are isolated from each other, and there are no covalent bonds between them; however, the shortest distance between them is less than the van der Waals diameter of the C_{60} molecule, and there are numerous $\text{C}\dots\text{C}$ contacts.

The Raman spectra were measured in the back-scattering geometry using a setup consisting of an Acton SpectraPro-2500i spectrograph with a Pixis2K CCD detector cooled to -70°C and an Olympus microscope. To excite Raman scattering, we used a continuous diode-pumped solid-state laser with $\lambda = 532$ nm. The laser beam was focused at the sample with an Olympus $10\times$ lens in a spot of ~ 2.6 μm in diameter. A large spot is necessary to lower the power density of laser radiation and to decrease the photopolymerization rate. The laser radiation line in the scattered beam was suppressed by an edge filter for $\lambda = 532$ nm with an absorbance of $\text{OD} = 6$ and a shift of the transmission bandwidth of ~ 100 cm^{-1} , and the laser excitation intensity just in front of the sample was ~ 100 μW . Measurements at high temperature were

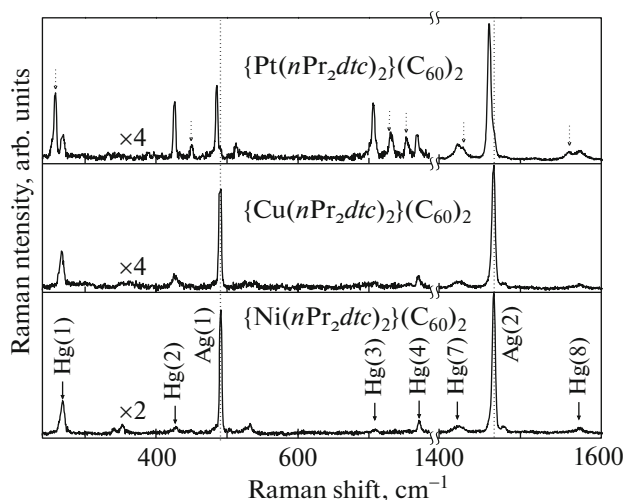


Fig. 1. Raman spectra of $\{\text{Ni}(n\text{Pr}_2\text{dte})_2\} \cdot (\text{C}_{60})_2$, $\{\text{Cu}(n\text{Pr}_2\text{dte})_2\} \cdot (\text{C}_{60})_2$, and $\{\text{Pt}(n\text{Pr}_2\text{dte})_2\} \cdot (\text{C}_{60})_2$ in the energy range of 240–1600 cm^{-1} at room temperature and normal pressure.

carried out using an optical cell, in which a Pt100 platinum thermometer was used as the temperature sensor, and the Termodat-08M3 electronic unit stabilized the temperature in the required range within $\pm 1.5^\circ\text{C}$.

3. RESULTS AND DISCUSSION

Figure 1 shows the Raman spectra of the $\{\text{Ni}(n\text{Pr}_2\text{dte})_2\} \cdot (\text{C}_{60})_2$, $\{\text{Cu}(n\text{Pr}_2\text{dte})_2\} \cdot (\text{C}_{60})_2$, and $\{\text{Pt}(n\text{Pr}_2\text{dte})_2\} \cdot (\text{C}_{60})_2$ complexes in the range of 240–1600 cm^{-1} at room temperature and normal pressure. All the spectra were measured at the same exposure times, wavelength, and laser radiation power. The bottom panel of the figure shows the spectrum of $\{\text{Ni}(n\text{Pr}_2\text{dte})_2\} \cdot (\text{C}_{60})_2$. The intensity of the phonon modes of molecular donors in the Raman spectra is smaller by orders of magnitude than the intensity of the C_{60} fullerene phonon modes, and they do not appear in the Raman spectra of complexes where the intramolecular phonon modes of C_{60} always dominate [7]. The vertical arrows on the bottom panel show the positions of Hg(1), Hg(3), Hg(4), Hg(7), Hg(8), Ag(1), and Ag(2) modes. The middle panel shows the Raman spectrum of the $\{\text{Cu}(n\text{Pr}_2\text{dte})_2\} \cdot (\text{C}_{60})_2$ complex, which does not differ from the spectrum of $\{\text{Ni}(n\text{Pr}_2\text{dte})_2\} \cdot (\text{C}_{60})_2$. The upper panel shows the Raman spectrum of $\{\text{Pt}(n\text{Pr}_2\text{dte})_2\} \cdot (\text{C}_{60})_2$: it clearly differs from the previous two both in the number of bands and in their position. Vertical lines indicate the position of Ag(1) and Ag(2) modes: they coincide on the lower two spectra, and on the upper spectrum, these modes are shifted towards lower energies, and weak satellites are seen to the right of them. In addition, the degenerate Hg(1), Hg(3), Hg(4), Hg(7), and

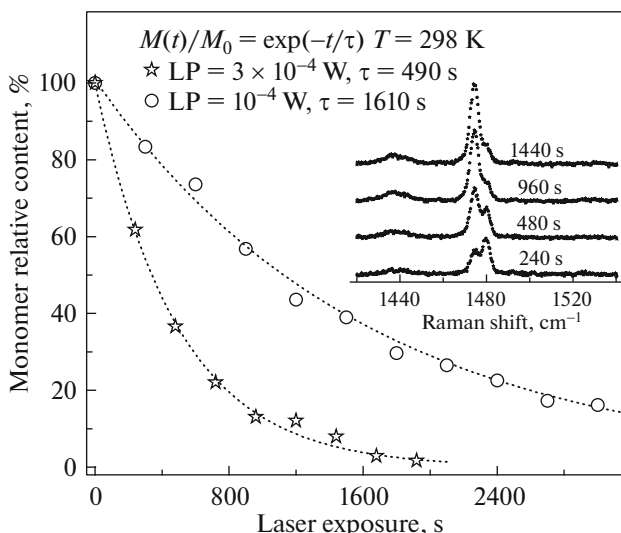


Fig. 2. Raman spectra of $\{\text{Pt}(n\text{Pr}_2\text{dte})_2\} \cdot (\text{C}_{60})_2$ in the region of the Ag(2) mode at room temperature and exposure for 240 s after 240, 480, 960, and 1440 s of continuous irradiation at a laser power of 300 μW . Dependence of the relative fraction of the monomer on the irradiation time at an excitation power of (stars) 300 and (circles) 100 μW ; (dotted curve) approximation of the experimental data by the exponential decay function.

Hg(8) modes are split, and the dashed arrows show the position of the new components. The changes in the Raman spectrum of $\{\text{Pt}(n\text{Pr}_2\text{dte})_2\} \cdot (\text{C}_{60})_2$ are similar to those that occur in the Raman spectra of fullerene photo- and crystalline polymers and are associated with the formation of covalent bonds between fullerene molecules in the complex layers [11, 13, 14].

The Raman spectra of the $\{\text{Pt}(n\text{Pr}_2\text{dte})_2\} \cdot (\text{C}_{60})_2$ complex in the region of the Ag(2) mode, recorded at room temperature in successively after 240, 480, 960, and 1440 s of continuous irradiation at a laser power of 300 μW and an exposure of 240 s are presented in Fig. 2. In the initial spectrum, the Ag(2) mode is represented by two bands: one at a frequency of $\sim 1469 \text{ cm}^{-1}$ corresponds to the C_{60} fullerene monomer, and another at a frequency of $\sim 1464 \text{ cm}^{-1}$ corresponds to the C_{120} fullerene dimer [18–20]. As the irradiation time increases, the intensity of the monomer band decreases, and the intensity of the dimer band increases and it dominates the Raman spectra at longer irradiation times. The relative fraction of the monomer versus the irradiation time, determined from the intensity ratio of the band at 1469 cm^{-1} to the sum of the intensities of both bands, is shown in Fig. 2 by stars, and the dotted curve is the approximation of the experimental data by the exponential decay function

$$M(t) = M_0 \exp(-t/\tau), \quad (1)$$

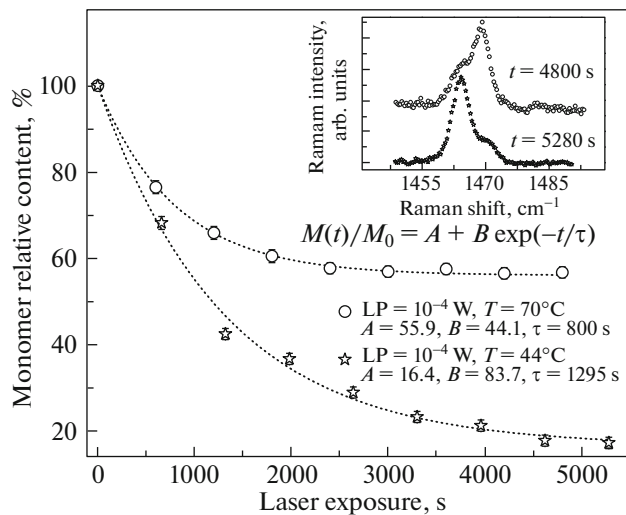


Fig. 3. Kinetics of photopolymerization in the fullerene layers of $\{\text{Pt}(\text{nPr}_2\text{dtc})_2\} \cdot (\text{C}_{60})_2$ at (stars) 44 and (circles) 70°C; (dotted curves) approximation of experimental data by the exponential decay function $M(t)/M_0 = A + B \exp(-t/\tau)$. Inset: Raman spectra of the complex at these temperatures after prolonged irradiation of the samples for 5280 and 4800 s.

where M_0 is the total number of C_{60} molecules in the irradiation spot at the depth of total absorption of laser radiation ($\sim 2 \mu\text{m}$ for $\lambda = 532 \text{ nm}$ [21]), and $\tau = 490 \text{ s}$ is the time constant. The circles in the figure show the similar dependence obtained at the laser power three times lower, $100 \mu\text{W}$, while the time constant $\tau = 1610 \text{ s}$ is greater by approximately three times. The photopolymerization rate should be directly proportional to the laser power density in the excitation spot, but slight differences in beam focusing and surface quality may lead to deviations from the exact proportionality over the light flux.

As is known, the free energy of fullerene polymers is lower than that of a fullerite crystal, and the states of the monomer and polymer are separated by an energy barrier. Therefore, the fullerene polymers are stable at room temperature, but they quickly break down at high temperatures [22, 23]. The thermal destruction of polymers accelerates with increasing temperature, and under constant irradiation, it competes with the current photopolymerization process. The kinetics of the formation of dimers at temperatures 44 and 70°C is shown in Fig. 3 by stars and circles, respectively, and the dotted curves are an approximation of these data by the exponential decay function

$$M(t)/M_0 = A + B \exp(-t/\tau), \quad (2)$$

where M_0 is the total number of C_{60} molecules in the irradiation spot, A and B are the residual quantity of monomer and dimer upon photopolymerization saturation, and τ is the time constant. The inset in Fig. 3 shows the Raman spectra measured at 44 and 70°C

after irradiation of the samples for 5280 and 4800 s; it is seen that the dimer concentration in the final product decreases with increasing temperature. The equilibrium between the formation of dimers and their thermal destruction occurs under the condition of

$$dD/dt = dM/dt = 0, \quad (3)$$

where D and M are the number of dimer and monomer molecules, and their total number in the excitation spot is constant, $M_0 = 2D + M$.

The thermal destruction of photopolymers in fullerene films was first studied by Raman scattering [24], and we follow the approach proposed in it in further discussion of our results. The change in the amount of dimers and monomers in the excitation spot on the irradiation time is determined by equations

$$\begin{aligned} dD/dt &= 1/2 K_p M - K_T D; \\ dM/dt &= -K_p M + 2K_T D, \end{aligned} \quad (4)$$

where K_p is the photopolymerization probability proportional to the light flux, and K_T is the probability of thermal destruction of the dimers. Taking into account the equilibrium condition (3) and the constancy of the number of molecules in the excitation spot, one can obtain

$$\begin{aligned} I_M &= M_0 \Sigma_M K_T / (K_p + K_T); \\ I_D &= M_0 \Sigma_D K_p / 2(K_p + K_T), \end{aligned} \quad (5)$$

where I_M and I_D are the intensities of the monomer and dimer bands in the Raman spectra, and Σ_M and Σ_D are the corresponding Raman cross sections. We believe that the rupture of the double $\text{C}=\text{C}$ bond in the C_{60} molecule does not lead to a change in the Raman scattering cross section, and $\Sigma_M \approx \Sigma_D$. Therefore, the intensity ratio of the dimer and monomer bands upon photopolymerization saturation is

$$I_D/I_M = 1/2 K_p / K_T. \quad (6)$$

The photopolymerization probability K_p can be estimated from the experimental dependence of the monomer fraction on the irradiation time. Fullerene polymers do not break down at room temperature of 295 K, and we can assume that $K_{295} \approx 0$. In this case, Eq. (4) takes the form $dM/dt = -K_p M$ or $M(t) = M_0 \exp(-K_p t)$, and the photopolymerization probability K_p is the reciprocal of the time constant $1/\tau$ and is $K_p = 6.21 \times 10^{-4} \text{ s}^{-1}$ at a laser power of $100 \mu\text{W}$.

The destruction of fullerene polymers is of an activation nature, and the temperature dependence of K_T is described by the Arrhenius equation

$$K_T = -A \exp(-E_A/K_B T), \quad (7)$$

where E_A is the activation energy, K_B is Boltzmann constant, and T is temperature [10, 23–25]. It follows from Eq. (7) that $\ln K_T = \ln(K_p/2) - \ln(I_D/I_M)$; therefore, the temperature dependence of K_T can be determined from the temperature dependence of the rela-

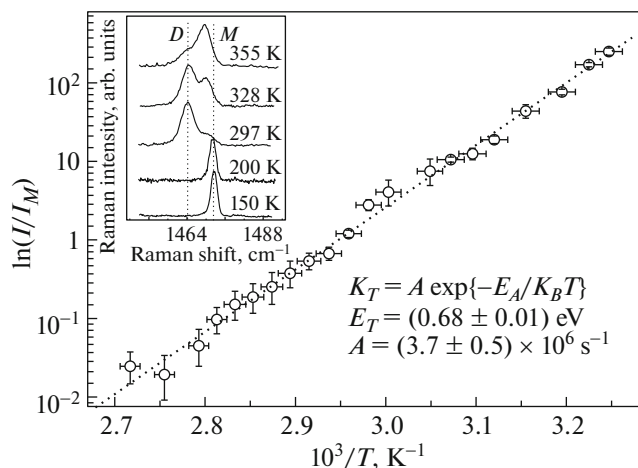


Fig. 4. Dependence of the relative intensity of dimer and monomer bands $\ln(I_D/I_M) = \ln(K_p/2) - \ln K_T$ on the inverse temperature $1000/T$, obtained from a series of measurements of Raman spectra under conditions of photopolymerization saturation: (circles) experimental data and (dotted line) approximation by linear dependence. Inset: Raman spectra of the complex at specific temperatures.

tive intensity of the dimer and monomer bands I_D/I_M under conditions of photopolymerization saturation. The dependence of the relative intensity of the dimer and monomer bands on the inverse temperature $1000/T$, obtained from a series of measurements of Raman spectra under conditions of photopolymerization saturation at temperatures from 35 to 95°C, is shown in Fig. 4 by circles. This dependence is well described in a logarithmic scale by a linear function (dotted line). The inset in Fig. 4 shows the Raman spectra of the complex at certain temperatures. We note that below 200 K, only the monomer band is represented in the spectra because at low temperatures, photopolymerization is not observed, as in fullerene crystals [18]. On the other hand, at a temperature above 355 K, the monomer band also dominates in the spectrum, which is associated with the rapid destruction of dimers. Using the obtained experimental data, it is possible to determine the constants in the Arrhenius equation (8), which make up $A = (3.7 \pm 0.5) \times 10^6 \text{ s}^{-1}$ and $E_A = (0.68 \pm 0.01) \text{ eV}$. They enable us to estimate the probability of destruction of photopolymers at room temperature as $K_{295} = 8.93 \times 10^{-6} \text{ s}^{-1}$. This value is approximately 70 times smaller than the photopolymerization probability $K_p = 6.21 \times 10^{-4} \text{ s}^{-1}$, which confirms the validity of our approximation of $K_{295} \approx 0$. The time of the destruction of the photopolymer to a concentration of 1%, calculated from the Arrhenius equation, is $5.16 \times 10^5 \text{ s}$ or approximately 6 days. We note that the lifetime of photooligomers in $\{\text{Pt}(\text{dbdtc})_2\} \cdot \text{C}_{60}$, determined earlier in [10], is approximately 326 days at room temperature. At the

same time, these values are many orders of magnitude smaller than the lifetime of the crystalline orthorhombic polymer of C_{60} fullerene, obtained by thermobaric treatment of fullerene at high pressure and temperature, which is hundreds of millions of years [25].

Another important parameter characterizing the stability of fullerene polymers is the temperature of their complete destruction, that is, the temperature at which they break down to 1% within 15 min. The destruction of crystalline fullerene polymers at this rate occurs in experiments on differential scanning calorimetry (DSC). The total destruction temperature determined by DSC is $\sim 260^\circ\text{C}$ for linear and planar polymers and $\sim 180^\circ\text{C}$ for fullerene dimers [22, 23, 26, 27]. Since the content of photopolymers in pure fullerene crystals and in fullerene molecular complexes is small, DSC is inapplicable in this case, but the total destruction temperature can be estimated from the Arrhenius equation. The temperature of complete destruction of photopolymers in fullerene crystals and films is approximately 185–190°C [24, 28]. For comparison, for fullerene photopolymers in $\{\text{Pt}(\text{dbdtc})_2\} \cdot \text{C}_{60}$, it is $\sim 130^\circ\text{C}$ [10], and, as measured in the present work, in $\{\text{Pt}(\text{nPr}_2\text{dtc})_2\} \cdot (\text{C}_{60})_2$, it is approximately 114°C. Thus, photopolymers in crystals of the donor–acceptor complexes of fullerene are less stable than the photo- and crystalline polymers of pure fullerene and are destroyed at lower temperatures. In most of the complexes studied (with the exception of complexes in which molecular donors contain platinum), photopolymerization in fullerene layers is observed only at high pressures, and a decrease in pressure leads to their immediate destruction even at room temperature [3, 4, 6, 8, 28]. The low stability of photopolymers in fullerene molecular complexes is connected, in our opinion, with the effect of layers of molecular donors that contribute to a more effective disruption of intermolecular bonds upon heating.

4. CONCLUSIONS

In the complex of fullerene with platinum bis(dipropyldithiocarbamate) $\{\text{Pt}(\text{nPr}_2\text{dtc})_2\} \cdot (\text{C}_{60})_2$, photopolymerization in fullerene layers is observed upon irradiation with visible laser light at normal pressure. The kinetics of photopolymerization at temperatures from room temperature to 110°C is studied, and it is shown that the thermal destruction of a photopolymer at high temperature leads to a decrease in its concentration in the final product obtained under conditions of photopolymerization saturation during prolonged irradiation. The dependence of the probability of destruction of a photopolymer on temperature is described by the Arrhenius equation $K_T = A \exp(-E_A/K_B T)$, with the activation energy $E_A = (0.68 \pm 0.03) \text{ eV}$ and $A = (3.7 \pm 0.5) \times 10^6 \text{ s}^{-1}$, and its total destruction to a concentration of 1% occurs within 15 min at $\sim 114^\circ\text{C}$. C_{60} photopolymers in

donor–acceptor complexes of fullerene are less stable at high temperatures than the photo- and crystalline polymers of fullerene.

ACKNOWLEDGMENTS

The author is grateful to D.V. Konarev for providing samples of fullerene molecular complexes.

The work is mainly supported by the Federal Agency of Scientific Organizations of the Russian Federation and partially supported by the Program of the Presidium of Russian Academy of Sciences “Condensed Matter Physics and New Generation Materials.”

REFERENCES

1. D. V. Konarev, A. Y. Kovalevsky, S. S. Khasanov, G. Saito, D. V. Lopatin, A. V. Umrikhin, A. Otsuka, and R. N. Lyubovskaya, *Eur. J. Inorg. Chem.*, 1881 (2006).
2. D. V. Konarev, S. S. Khasanov, A. Otsuka, M. Maesato, S. Gunzi, and R. N. Lyubovskaya, *Angew. Chem.* **49**, 4829 (2010).
3. W. Cui, M. Yao, D. Liu, Q. Li, R. Liu, B. Zou, T. Cui, and B. Liu, *J. Phys. Chem. B* **116**, 2643 (2012).
4. K. Kato, H. Murata, H. Gonnokami, and M. Tacibana, *Carbon* **107**, 622 (2016).
5. S. Sun, W. Gui, S. Wang, and B. Liu, *Sci. Rep.* **7**, 10809 (2017).
6. K. P. Meletov, V. K. Dolganov, N. G. Spitsina, E. B. Yagubskii, J. Arvanitidis, K. Papagelis, S. Ves, and G. Kourouklis, *Chem. Phys. Lett.* **281**, 360 (1997).
7. K. P. Meletov, *Phys. Solid State* **56**, 1689 (2014).
8. K. P. Meletov, D. V. Konarev, and A. O. Tolstikova, *J. Exp. Theor. Phys.* **120**, 989 (2015).
9. A. V. Kuzmin, D. V. Konarev, S. S. Khasanov, and K. P. Meletov, *Nanosyst.: Phys. Chem. Math.* **9**, 33 (2018).
10. K. P. Meletov, G. Velkos, J. Arvanitidis, D. Christofilos, and G. A. Kourouklis, *Chem. Phys. Lett.* **681**, 124 (2017).
11. F. M. Rao, P. Zhou, K.-A. Wang, G. T. Hager, J. M. Holden, Y. Wang, W.-T. Lee, X.-X. Bi, P. C. Eklund, D. S. Cornett, M. A. Duncan, and I. J. Amster, *Science* (Washington, DC, U. S.) **259**, 955 (1993).
12. J. Winter and H. Kuzmany, *Solid State Commun.* **84**, 935 (1992).
13. P. W. Stephens, G. Bortel, G. Faigel, M. Tegze, A. Janossy, S. Pekker, G. Oszlanyi, and L. Forro, *Nature* (London, U.K.) **370**, 636 (1994).
14. Y. Iwasa, T. Arima, R. M. Fleming, T. Siegrist, O. Zhou, R. C. Haddon, L. J. Rothberg, K. B. Lyons, H. L. Carter, A. F. Hebard, R. Tycko, G. Dabbagh, J. J. Krajewski, G. A. Thomas, and T. Yagi, *Science* (Washington, DC, U. S.) **264**, 1570 (1994).
15. M. Nunez-Regueiro, L. Marques, J.-L. Hodeau, O. Bethoux, and M. Perroux, *Phys. Rev. Lett.* **74**, 278 (1995).
16. K. P. Meletov and G. A. Kourouklis, *J. Exp. Theor. Phys.* **115**, 707 (2012).
17. D. V. Konarev, S. S. Khasanov, D. V. Lopatin, V. V. Rodaev, and R. N. Lyubovskaya, *Russ. Chem. Bull.* **56**, 2145 (2007).
18. Ping Zhou, Zheng-Hong Dong, A. M. Rao, and P. C. Eklund, *Chem. Phys. Lett.* **211**, 337 (1993).
19. T. Wägberg, P.-A. Persson, B. Sundqvist, and P. Jacobsson, *Appl. Phys. A* **64**, 223 (1997).
20. S. Lebedkin, A. Gromov, S. Giesa, R. Gleiter, B. Renker, H. Rietschel, and W. Kräthmer, *Chem. Phys. Lett.* **285**, 210 (1998).
21. K. P. Meletov, V. K. Dolganov, O. V. Zharikov, I. N. Kremenskaya, and Yu. A. Ossipyan, *J. Phys. I* **2**, 2097 (1992).
22. Y. Iwasa, K. Tanoue, T. Mitani, and T. Yagi, *Phys. Rev. B* **58**, 16374 (1998).
23. P. Nagel, V. Pasler, S. Lebedkin, A. Soldatov, C. Meingast, B. Sundqvist, P.-A. Persson, T. Tanaka, K. Komatsu, S. Buga, and A. Inaba, *Phys. Rev. B* **60**, 16920 (1999).
24. Ying Wang, J. M. Holden, Xiang-xin Bi, and P. C. Eklund, *Chem. Phys. Lett.* **217**, 413 (1994).
25. K. P. Meletov, J. Arvanitidis, D. Christofilos, G. A. Kourouklis, Y. Iwasa, and S. Yamanaka, *Carbon* **48**, 2974 (2010).
26. M. V. Korobov, A. G. Bogachev, A. A. Popov, V. M. Senyavin, E. B. Stukalin, A. V. Dzyabchenko, V. A. Davydov, L. S. Kashevarova, A. V. Rakhmanina, and V. Agafonov, *Carbon* **43**, 954 (2005).
27. G.-Wu Wang, K. Komatsu, Y. Murata, and M. Shiro, *Nature* (London, U.K.) **387**, 583 (1997).
28. K. P. Meletov, J. Arvanitidis, D. Christofilos, G. Kourouklis, and V. A. Davydov, *Nanosyst.: Phys. Chem. Math.* **9**, 29 (2018).

Translated by O. Zhukova